

# Topological phase diagrams of the frustrated Ising ferromagnet

Alejandro Mendoza-Coto,<sup>1,\*</sup> Danilo Emanuel Barreto de Oliveira,<sup>2</sup> Lucas Nicolao,<sup>1</sup> and Rogelio Díaz-Méndez<sup>3</sup>

<sup>1</sup>*Departamento de Física, Universidade Federal de Santa Catarina, 88040-900 Florianópolis, Brazil*

<sup>2</sup>*Departamento de Física, Universidade Federal de Rio Grande do Sul, 91501-970 Porto Alegre, Brazil*

<sup>3</sup>*Department of Physics, KTH Royal Institute of Technology, SE-10691 Stockholm, Sweden*

(Dated: June 24, 2022)

The emergence of complex modulated structures in the magnetization pattern of thin films is a well-established experimental phenomenology caused by the frustrating effects of competing interactions. Using a coarse-grained version of the Ising ferromagnet with dipolar interactions, we develop a method that use the information from the microscopic Hamiltonian to predict the specific topology of these phases. This is done with a combination of the mean-field phase diagrams obtained by minimization of the free energy functional, and the classical theory of melting. In this frame we are able to clearly distinguish orientational and translational symmetry and discriminate between the long and short range ordering of the system for all temperatures and fields. We observe that the reentrance developed by the  $H$ - $T$  phase diagrams in the regime of weak dipolar interactions is directly related with the appearance of anomalous topological transitions. These results motivate the realization of new experiments on magnetic thin films allowing to determine the connection between the reentrance and the behavior of the topological phases in real materials.

PACS numbers:

Keywords: Topological phases, Frustrated ferromagnet, Reentrant behavior

## I. INTRODUCTION

The complex patterned phases appearing in two dimensional systems with competing interaction have been extensively studied in the literature<sup>1-7</sup>. The interest in such systems goes beyond the technological relevance. Since in two dimensions the fluctuations can be particularly strong even at very low temperature, systems are usually unable to stabilize crystalline patterns and consequently only weaker forms of order are observed<sup>8-11</sup>. Example of these phases are the nematic phase in two dimensional systems of stripes, and the smectic and hexatic phases in two dimensional systems of particles<sup>12-16</sup>. Theoretically speaking, the melting of these phases is expected to occur through some topological mechanism with increasing temperature<sup>17</sup>.

A model system presenting this phenomenology is the so-called isotropic dipolar ferromagnet with strong perpendicular anisotropy<sup>18-22</sup>. In this model the competition between the ferromagnetic interaction and the dipolar antiferromagnetic interaction produce nontrivial magnetic textures of the out-of-plane magnetization. For this scenario a commonly observed structure is the stripe configuration, in which the sign of the local magnetization oscillates when moving along a given direction in the system. According to the Kosterlitz-Thouless-Halperin-Nelson-Young (KTHNY) classical theory of melting<sup>23-25</sup>, this stripe phase posses only local positional order, though a weak orientational order is stable with power-law decaying correlations. The latter is usually called the nematic phase. Upon increasing temperature this nematic phase melts into a liquid of stripes with only local positional and orientational order.

Although several works have considered the properties of these transitions, fewer attempts have been made to characterize the properties of the nematic transition when an external magnetic field is applied. The external field naturally favors magnetic domains oriented along its direction, producing an enlargement of the modulation length and an asymmetry of the positive and negative domains in the stripe pattern. These effects are very hard to relate with the topological properties of the stripe phase on physical grounds, which explain the lack of literature on the detailed characterization of the topological phases within the stripe region.

A similar situation is present regarding the topological properties of the bubble phase observed for larger fields. Although experimentally and computationally accessible, a topological characterization of the bubble lattice varying temperature and magnetic field is still lacking. While it can be argued that perfect bubble configurations share the same symmetries of a triangular lattice of particles, it is not clear whether the elastic effective Hamiltonian of the bubble patterns coincide with that of a triangular crystal. Consequently, the topological phases and its behavior within the bubble region of the  $H$ - $T$  phase diagram, although possibly related somehow to the problem of the two dimensional melting of triangular crystals, lacks of theoretical description.

Another intriguing issue is the effect produced on the topological phases due to the presence of reentrance in the phase diagrams. Systems like the dipolar ferromagnet can present strong reentrances in the  $H$ - $T$  plane, depending on the relative strength of the dipolar and the ferromagnetic interactions<sup>26</sup>. For systems with weak enough repulsive interaction the  $H$ - $T$  phase diagram develops an inverse melting in a certain range of the external field. This anomaly in the phase diagram is accompanied by an anomalous behavior of the Young modulus of the patterns, which suggests possible modifications in the topological order of the magnetic texture.

In this work we present a method that use the information from the microscopic Hamiltonian of a coarse-grained Ising model with dipolar interactions to predict the specific type of pattern that emerges at any value of  $H$  and  $T$ . Minimizing the mean-field

free energy functional and combining with the classical theory of melting, we show that it is possible to identify the long or short range nature of the orientational and positional order. This allows to correctly understand both the effect of an external field in the topology of the system and the role of the reentrance of the  $H$ - $T$  phase diagrams in the appearance of anomalous topological transitions.

This paper is organized as follows. In sections two and three the microscopic model is described and the mean-field free energy functional is built, to be used as starting point in obtaining the elastic and topological properties of the different mesophases. In section four we discuss the numerical results on the topological phase diagrams varying the relative strength of the dipolar interaction. Section five focuses on the characterization of some critical properties of the topological transitions between the different phases. The general conclusions are discussed in section six.

## II. MODEL

We begin considering a 2D Ising spin model with nearest-neighbor ferromagnetic coupling  $J$  and a long-range dipolar interaction of relative strength  $\delta^{-1}$ . This model can be described by the Hamiltonian<sup>27,28</sup>

$$\mathcal{H} = -\frac{J}{2} \sum_{\langle i,j \rangle} s_i s_j + \frac{J}{2\delta} \sum_{i \neq j} \frac{s_i s_j}{|\vec{x}_i - \vec{x}_j|^3} - h \sum_i s_i, \quad (1)$$

where  $h$  represents the external magnetic field applied perpendicular to the plane of the system. In the Fourier space the previous expression can be rewritten as

$$\mathcal{H} = \frac{1}{2} \int_{BZ} \frac{d^2 \vec{k}}{(2\pi)^2} \hat{A}(k) \hat{s}(\vec{k}) \hat{s}(-\vec{k}) - \int_{BZ} \frac{d^2 k}{(2\pi)^2} h(k) \hat{s}(-k), \quad (2)$$

where the function  $\hat{A}(k)$  represent the so called fluctuation spectrum and the subindex “ $BZ$ ” stands for the first Brillouin zone of the original square lattice. The fluctuation spectrum in the long wave limit  $k \rightarrow 0$ , as obtained by Cannas et. al.<sup>27</sup> will be given approximately by the expression

$$\begin{aligned} \hat{A}(k) &= -2J \left( 2 - \frac{k^2}{2} \right) + \frac{J}{\delta} \left( \frac{2\pi^2}{3} + 2\zeta(3) - 2\pi k + k^2 \right) \\ &= -\frac{(6\zeta(3) - \pi^2 + 2\delta(\pi^2 + 3\zeta(3) - 6) - 12\delta^2)}{3\delta(1 + \delta)} J + \frac{1 + \delta}{\delta} J \left( k - \frac{\pi}{1 + \delta} \right)^2. \end{aligned}$$

Following standard procedures the mean field free energy of the system in the continuum limit is given by<sup>26,29</sup>

$$\mathcal{F}[\phi] = \frac{1}{2} \int \frac{d^2 \vec{k}}{(2\pi)^2} \hat{A}(k) \hat{\phi}(\vec{k}) \hat{\phi}(-\vec{k}) + KT \int d^2 x S(\phi) - h \int d^2 \vec{x} \phi(\vec{x}),$$

where  $S(\phi) = \frac{(1+\phi)}{2} \log \left( \frac{(1+\phi)}{2} \right) + \frac{(1-\phi)}{2} \log \left( \frac{(1-\phi)}{2} \right)$  represent the local mean field entropy of the Ising model. Now we proceed with the construction of the dimensionless variational free energy, appropriate for the numerical analysis. The re-scaling of momenta and lengths are taken in the form  $\vec{k}/k_0 = \vec{k}'$  and  $k_0 \vec{x} = \vec{x}'$ , which leads to a re-scaling of the Fourier transforms as  $\hat{\phi}'(\vec{k}') = k_0^2 \hat{\phi}(\vec{k}/k_0)$ . With the new variables, the original free energy functional can be written in terms of the field  $\phi(\vec{x}')$  as

$$\mathcal{F}[\phi'] = \frac{\hat{A}(k_0)}{k_0^2} \left[ \frac{1}{2} \int \frac{d^2 \vec{k}'}{(2\pi)^2} \hat{A}'(k') \hat{\phi}'(\vec{k}') \hat{\phi}'(-\vec{k}') + T' \int d^2 \vec{x}' S(\phi'(\vec{x}')) - h' \int d^2 \vec{x}' \phi(\vec{x}') \right]$$

where

$$A'(\vec{k}') = -1 + a(k-1)^2 \quad (3)$$

$$a = 3\pi^2 / (\pi^2 - 6\zeta(3) + 2\delta(6 - \pi^2 - 3\zeta(3)) + 12\delta^2) \quad (4)$$

$$T' = KT / \hat{A}(k_0) \quad (5)$$

$$h' = h / \hat{A}(k_0) \quad (6)$$

Finally we choose the units of energy as the quantity  $\hat{A}(k_0)/k_0^2$ , which leads to the dimensionless free energy functional<sup>26,29</sup>

$$\mathcal{F}[\phi] = \frac{1}{2} \int \frac{d^2 \vec{k}}{(2\pi)^2} \hat{A}(k) \hat{\phi}(\vec{k}) \hat{\phi}(-\vec{k}) + T \int d^2 \vec{x} S(\phi(\vec{x})) - h \int d^2 \vec{x} \phi(\vec{x}), \quad (7)$$

where prime symbols have been omitted to simplify the notation.

This kind of mean field free energy have been extensively used as a starting point to construct the phase diagram of systems with competing interactions by looking at the local structure of the order parameter<sup>26</sup>. However, when the phases need to be distinguished by its symmetries, the desired phase diagram should contain information about the translational and rotational order of the different textures the magnetic system develops. In this case a simple discrimination in terms of stripe, bubble and homogeneous phases is no longer sufficient. While in the mean-field context the modulated phases represent perfectly ordered states, it is well-known that in two dimensions the fluctuations destabilize these perfect configurations. The accepted interpretation is that mean-field results give information only about the local structure of the order parameter and not about the symmetries of the pattern under consideration.

### III. TOPOLOGICAL PHASES

In order to find a more accurate description of the phase diagram of systems with competing interactions we must include the role of the topological fluctuations of the different textures. As it is well-known from KTHNY theory, these are the most relevant fluctuations in the melting of modulated patterns. This theory concludes that isotropic two-dimensional stripe systems can at best break the rotational symmetry into a nematic phase at low temperatures. Upon heating, this nematic phase will eventually melt into a disordered phase in which both the positional and the orientational order exist only locally.

On the other hand it is expected that, if the bubble structure behaves as a triangular lattice of particles, it could in principle melt following a sequence of smectic, hexatic and liquid phases as temperature is increased from the low temperature regime. As usual, in the smectic phase the system should exhibit quasi-long-range positional order and long-range orientational order; in the hexatic phase, local positional order and quasi-long-range orientational order; and in the liquid of bubbles local positional and orientational order.

To study the topological order of the modulated structures we use as starting point the free energy functional of Eq. (7) as our effective coarse grained Hamiltonian depending on the local order parameter  $\phi(\vec{x})$ . By allowing fluctuations in the wave phase of the different modulations that minimize this effective Hamiltonian we then obtain the effective *elastic* Hamiltonian for each modulated optimized pattern. The elastic Hamiltonians are consistent with those of KTHNY theory, and consequently can be used as the starting point for a Renormalization Group (RG) analysis of the type performed in the classical theory of melting. The latter ultimately allows to calculate the topological properties of the system at any point in the phase diagram.

#### A. Topological characterization of the stripe phase

As discussed in the literature<sup>26</sup>, one of the possible configurations minimizing a free energy functional of the form of Eq. (7) is a periodic modulation in one direction, i.e. the stripe solution. When allowing fluctuations in the wave phase of this solution, the local order parameter takes the form

$$\phi(\vec{x}) = c_0 + \sum_{n=1}^{\infty} c_n \cos(nk_0 x + nk_0 u(\vec{x})) \quad (8)$$

where  $u(\vec{x})$  represent the deformation field of the stripes and  $\vec{x}$  is the direction transversal to the the average orientation of the stripes. Setting the deformation field of the stripes  $u(\vec{x})$  to a constant, the variational free energy of Eq. (7) remains invariant as expected. Substituting the proposed anzats in the variational free energy the elastic effective Hamiltonian, up to second order in  $\hat{u}(\vec{k})$ , will be<sup>11,12,15,30</sup>

$$\mathcal{F}[\phi] = \mathcal{F}[\phi_0] + \frac{1}{2} \int \frac{d^2 \vec{k}}{(2\pi)^2} \hat{B}(\vec{k}) \hat{u}(\vec{k}) \hat{u}(-\vec{k}) \quad (9)$$

where

$$\hat{B}(\vec{k}) = B(k_x^2 + \lambda^2 k_y^4) \quad (10)$$

and

$$B = \frac{1}{2!} \frac{\partial^2}{\partial k_x^2} \left( \sum_{n=1}^{\infty} \frac{c_n^2 n^2 k_0^2}{4} \left[ \hat{A}(\vec{k} - n\vec{k}_0) + \hat{A}(\vec{k} + n\vec{k}_0) \right] \right) \Big|_{\vec{k} \rightarrow 0} \quad (11)$$

$$B\lambda^2 = \frac{1}{4!} \frac{\partial^4}{\partial k_y^4} \left( \sum_{n=1}^{\infty} \frac{c_n^2 n^2 k_0^2}{4} \left[ \hat{A}(\vec{k} - n\vec{k}_0) + \hat{A}(\vec{k} + n\vec{k}_0) \right] \right) \Big|_{\vec{k} \rightarrow 0} \quad (12)$$

The elastic Hamiltonian given in Eq. (9) is just the starting point of the analysis of the topological melting of a system of stripes as discussed by Toner and Nelson<sup>11</sup>. The main consequence of the specific form of the elastic Hamiltonian obtained is the divergence of  $\langle u^2(\vec{x}) \rangle$ , which implies that the stripe order is unstable in two dimensions. At the same time, a careful analysis of the fluctuations of the stripe orientation  $\theta(x) = \partial_y u(x)$  allows to conclude that at low temperature the system has a phase with quasi-long-range orientational order, characterized by power law decaying orientational correlations. The presence of such a weak orientational order at low temperature is a consequence of the presence of topological defects (dislocations) in the stripe structure. This scenario is coherent with an effective orientational Hamiltonian of the form

$$\Delta H_{ef} = \frac{1}{2} \int d^2x K (\vec{\nabla} \theta(\vec{x}))^2. \quad (13)$$

The effective orientational stiffness ( $K$ ) can be approximated by<sup>11</sup>

$$K = \frac{B\lambda^2 + 2E_d}{2}, \quad (14)$$

where  $E_d$  represents the energy of a dislocation and can be estimated to be  $E_d = \pi B \lambda^{1/2} k_0^{-3/231}$ . The RG equations for the XY effective model are known to be

$$\begin{aligned} \frac{dK}{dl} &= -4\pi^3 K(l)^2 y(l) \\ \frac{dy}{dl} &= (2 - \pi K(l)) y(l), \end{aligned} \quad (15)$$

where the bare quantities are given by  $y(0) = \exp(-E_c/k_B T)$  and  $K(0) = K/k_B T$ . The energy of the relevant topological defects (disclinations) can be estimated by a technique equivalent to that used by Abanov et al.<sup>12</sup> to be  $E_c = K\pi(\gamma - \text{cosintegral}(\pi) + \ln(\pi))$ .

Equations (11-15) allow the calculation of the renormalized stiffness, which is used to identify the orientational transition as the point at which  $K(+\infty)$  goes to zero. This transition between a quasi-long-range orientationally ordered stripe phase and the stripe liquid is the so-called nematic transition<sup>13</sup>.

## B. Topological characterization of the bubble phase

Now the equivalent analysis is described for the bubble configurations. An analytical study of the topological order of the bubble pattern, to the best of our knowledge, is not currently available in the literature. Nevertheless, the same principles of the classical melting theory of stripes can be generalized to this case.

We start by deducing the elastic Hamiltonian of the bubble pattern in the limit of small deformations. In this case we admit that the deformation field must be a two component vectorial field. In order to allow only deformation fields that respect locally the symmetries of the bubble pattern we consider the following form of the modulation in the presence of fluctuations

$$\phi(\vec{x}) = c_0 + \sum_{n=1}^{\infty} c_n \cos(k_0 \vec{b}_n \cdot \vec{x} + k_0 \vec{b}_n \cdot \vec{u}(\vec{x})), \quad (16)$$

where  $\vec{u}(\vec{x})$  represents the deformation field of the bubble configuration. Analogous to the stripe case, the free energy of the pattern remains invariant if the field  $\vec{u}(\vec{x})$  is set to a constant. Following a procedure similar to the one described in the previous subsection it is straightforward to reach the following elastic Hamiltonian for the bubble system

$$\begin{aligned} \mathcal{F}[\phi] &= \mathcal{F}[\phi_0] + \frac{1}{2} \int \frac{d^2 \vec{k}}{(2\pi)^2} ((2m+l)k_x^2 + mk_y^2) \hat{u}_x(\vec{k}) \hat{u}_x(-\vec{k}) \\ &+ \frac{1}{2} \int \frac{d^2 \vec{k}}{(2\pi)^2} ((2m+l)k_y^2 + mk_x^2) \hat{u}_y(\vec{k}) \hat{u}_y(-\vec{k}) + \frac{1}{2} \int \frac{d^2 \vec{k}}{(2\pi)^2} (2m+2l) k_x k_y \hat{u}_x(\vec{k}) \hat{u}_y(-\vec{k}), \end{aligned} \quad (17)$$

where the elastic stiffnesses  $m$  and  $l$  can be calculated by solving the following system of equations

$$\begin{aligned} 2m + l &= \frac{1}{2!} \frac{\partial^2}{\partial k_x^2} \left( \sum_{n=1}^{\infty} \frac{c_n^2 k_0^2 (b_n^x)^2}{4} \left[ \hat{A}(\vec{k} - k_0 \vec{b}_n) + \hat{A}(\vec{k} + k_0 \vec{b}_n) \right] \right) \Big|_{\vec{k} \rightarrow 0}, \\ m &= \frac{1}{2!} \frac{\partial^2}{\partial k_y^2} \left( \sum_{n=1}^{\infty} \frac{c_n^2 k_0^2 (b_n^x)^2}{4} \left[ \hat{A}(\vec{k} - k_0 \vec{b}_n) + \hat{A}(\vec{k} + k_0 \vec{b}_n) \right] \right) \Big|_{\vec{k} \rightarrow 0}. \end{aligned} \quad (18)$$

The above effective Hamiltonian has the form of the elastic Hamiltonian of a triangular crystal in two dimensions. This implies that the triangular array of bubbles can be treated like a triangular lattice of particles, with Lamé's elastic coefficients given by the expressions in Eq. (18). It implies that the topological properties of the bubble lattice can be studied using the results from KTHNY theory.

The KTHNY theory predicts that in two dimensions the triangular lattice of particles melts by a sequence of two transitions. At low temperature, the triangular lattice of particles (bubbles) is in the so-called smectic phase, a state in which positional correlation decays as a power law and the bond angle presents long-range order. Upon increasing the temperature a transition is predicted to an intermediate phase usually called a hexatic phase, characterized by exponentially decaying positional correlations and power-law bond angle orientational correlations. Finally a further increase of the temperature leads the system to a liquid state in which the positional and the bond angle orientational order are both short ranged.

### 1. Smectic transition

The smectic transition is mediated by the proliferation of dislocation pairs<sup>17</sup>. The effective Hamiltonian of the interacting dislocation field is given by the expression

$$\Delta H_D = -\frac{K_d}{8\pi a^4} \int d^2x d^2x' \left[ \vec{b}(\vec{x}) \cdot \vec{b}(\vec{x}') \ln \left( \frac{|\vec{x} - \vec{x}'|}{a} \right) - \frac{\vec{b}(\vec{x}) \cdot (\vec{x} - \vec{x}') \vec{b}(\vec{x}') \cdot (\vec{x} - \vec{x}')}{|\vec{x} - \vec{x}'|^2} \right] + E_c \int \frac{d^2x}{a^2} |\vec{b}(\vec{x})|^2, \quad (19)$$

where  $a$  represents the short distance cut-off of the interacting dislocation problem, which could be interpreted as the minimum possible distance in a dislocation pair. The elastic constant  $K_d$  is given by  $\frac{4m(m+l)}{(2m+l)} \left( \frac{4\pi}{\sqrt{3}k_0} \right)^2$  and the parameter  $E_c$  represents the energy of a dislocation. Since the energy of a single dislocation diverges,  $E_c$  have to be understood as half the minimum energy of a dislocation pair. To estimate the value of the energy of a dislocation pair we applied a technique similar to the one used by Abanov et al.<sup>31</sup>. First, the interacting part of the Hamiltonian of Eq. (19) is written in Fourier space, and a configuration of Burguer's vectors of the dislocation pair is selected by minimizing the interaction energy. Then the calculation is performed directly in Fourier space properly selecting the momentum cut-off. This procedure leads to the result  $E_c = K_d(\gamma - \text{cosintegral}(\pi) + \ln(\pi))/(8\pi)$ . The relation group equations for the renormalized stiffness is

$$\frac{dK_s(l)}{dl} = -K_s^2(l) \left[ \frac{3\pi}{2} y(l)^2 \exp(K_s(l)/8\pi) I_0(K_s(l)/8\pi) - \frac{3\pi}{4} y(l)^2 \exp(K_s(l)/8\pi) I_1(K_s(l)/8\pi) \right] \quad (20)$$

$$\frac{dy(l)}{dl} = \left( 2 - \frac{K_s(l)}{8\pi} \right) y(l) + 2\pi y(l)^2 \exp(K_s(l)/8\pi) I_0(K_s(l)/16\pi), \quad (21)$$

where  $K_s(0) = K_d/k_B T$  and  $y(0) = \exp(-E_c/k_B T)$ . The integration of this system of differential equations allows to identify when the transition from the smectic to the hexatic phase takes place. We define the smectic phase region as composed by those points satisfying that  $K_d(+\infty)$  is finite. The integration of the RG equations in the regions where the positional order is only local ( $K_d(+\infty) = 0$ ) allows the determination of the positional correlation length in units of the short distance cut-off ( $\xi_p/a$ ). As it is well established in the RG theory  $\xi_p/a$  can be calculated as  $\exp(l^*)$ , where  $l^*$  represents the RG time to  $K_d(l)$  reach  $K_d(+\infty)$ . Normally  $K_d(l)$  have a very steep evolution so it is relatively easy to identify  $l^*$ . In this way the positional correlation can be calculated, which as discussed below is a central quantity for the characterization of the orientational order.

### 2. Hexatic transition

As we mentioned before once the smectic phase melts the system can develop an hexatic or a liquid phase. In this region of the phase diagram the orientational order, according to the classical theory of melting, can be effectively described by a Hamiltonian of the form

$$\Delta H_o = \frac{1}{2} \int d^2x K_A (\vec{\nabla} \theta(\vec{x}))^2 \quad (22)$$

where the so-called Frank's constant  $K_A$  is normally estimated to be  $2E_c(\xi_p/a)^{217,24}$ . Since the effective model describing the orientational order in the long wave limit coincides with the  $XY$  model, we can take advantage of the well known RG equations for the elastic constant  $K_A$ . This system of equations have the form

$$\frac{dK_h(l)}{dl} = -4\pi^3 K_h(l)^2 y^2(l) \quad (23)$$

$$\frac{dy(l)}{dl} = (2 - \pi K_h(l))y(l), \quad (24)$$

where the bare elastic constant  $K_h(0)$  is given by  $K_A/k_B T$  and the bare fugacity  $y(0)$  is taken as usual  $\exp(-E_A/k_B T)$ , with  $E_A$  representing the energy of the relevant topological defects (disclinations) of this transition. The energy of the disclinations can be estimated in a form equivalent to the one used for calculating the energy of a dislocation in the previous section. Following that procedure we reach to  $E_A = K_A \pi (\gamma - \text{cosintegral}(\pi) + \ln(\pi))/36$ . This result completes the set of equations for characterizing the orientational order of the bubble phase. The set of equations obtained in this section allows to identify the melting temperature of the hexatic phase as the one in which the renormalized orientational stiffness  $K(+\infty)$  goes to zero.

#### IV. TOPOLOGICAL PHASE DIAGRAMS

The numerical procedure for the construction of the topological phase diagram can be outlined as follows. First the free energy functional of Eq. (7) is minimized, which allows to find the optimal stripe and bubble solution. These results are then used to calculate the Lamé's coefficients ( $B$ ,  $B\lambda^2$ ,  $m$ ,  $2m + l$ ) for the stripes and bubbles. The knowledge of these quantities is the starting point for the application of the classical theory of melting described in previous sections, which ultimately allows to establish the topological order of a given pattern.

Following this procedure we construct several  $H$ - $T$  phase diagrams varying the curvature of the fluctuation spectrum  $a$  in Eq. (7). As can be noticed in the definition of the model, different values of the parameter  $a$  are equivalent to different relative strengths of the dipolar interaction  $\delta^{-1}$  in the microscopic Hamiltonian of Eq. (1). As studied in previous works, varying the curvature of the fluctuation spectrum this system develops a strong reentrance of the homogeneous phase with temperature<sup>26</sup>. However, to the best of our knowledge this type of topological phase diagrams have not been obtained before, and consequently a number of interesting questions like the influence of the reentrance in the topological properties of the system remains open.

In Fig. 1 a sequence of  $H$ - $T$  topological phase diagrams is presented varying the curvature of the fluctuation spectrum  $a$  from a regime with practically zero reentrance to a regime of strong reentrance. The first thing we notice for all diagrams is that, depending on the value of the magnetic field, the sequence of transitions is not always the one predicted by the classical theory of melting. This happens not only due to the relative change of stability between modulated phases, but also because of the occurrence of direct transitions from the modulated to the disordered phase. This kind of transitions are beyond the scope of the classical theory of melting and are obtained here as a result of the simultaneous use of a density functional theory and the RG techniques, providing a richer outcome than that produced by each technique separately.

The sequence of phase diagrams in Fig. 1 shows that decreasing the relative strength of the dipolar interaction  $\delta^{-1}$ , the development of reentrance in the phase diagram produces continuously a qualitative transformation of the topological phases, specifically of the boundary between different phases. In the absence of reentrance, the boundaries of the topological phases are given by monotonous decreasing curves in the  $H$ - $T$  plane. This is the behavior expected in a normal phase diagram since the intuition suggests that the application of an external magnetic field weakens the modulations and consequently these phases are less pronounced. However, we observe that, as the homogeneous reentrance becomes stronger, the boundaries of the topological phases develop a non-monotonic behavior. This tendency is responsible for the eventual appearance of unexpected reentrances of the topological phases when the magnetic field is increased at constant temperature. See for instance the phase diagram presented for the lowest value of the parameter  $a$  ( $a = 0.5$ ), in this case increasing the magnetic field a reentrance appears in the boundaries of all topological phases.

In our level of approximation, all topological transitions within the bubble or within the stripe mean-field region occur at a fixed value of the relevant stiffness, normalized by the thermal energies ( $K(0)$ ,  $K_s(0)$ ,  $K_h(0)$ ). If we trace back the dependence of these quantities with the microscopic parameters we find a relation of proportionality with the microscopic elastic coefficients ( $B$ ,  $B\lambda^2$ ,  $m$ ,  $2m + l$ ) and with the modulation length ( $2\pi/k_0$ ). A numerical analysis of the behavior of these quantities in the region of the boundaries of the topological phases reveals that in all cases, as expected, when the external field is increased, the microscopic elastic coefficients decrease as modulations become less pronounced. At the same time, however, the modulation length of the patterns is a quantity that increases with increasing the external field. This scenario suggests that the non trivial behavior of the topological phase boundaries is mainly a consequence of the behavior of the modulation length when increasing the external field in the cases with homogeneous reentrance. We identify that for these topological reentrances the modulation length of the pattern grows with the external field fast enough to overcome the effect of the decreasing microscopic elastic coefficients, making finally the relevant stiffnesses to increase with the external field.

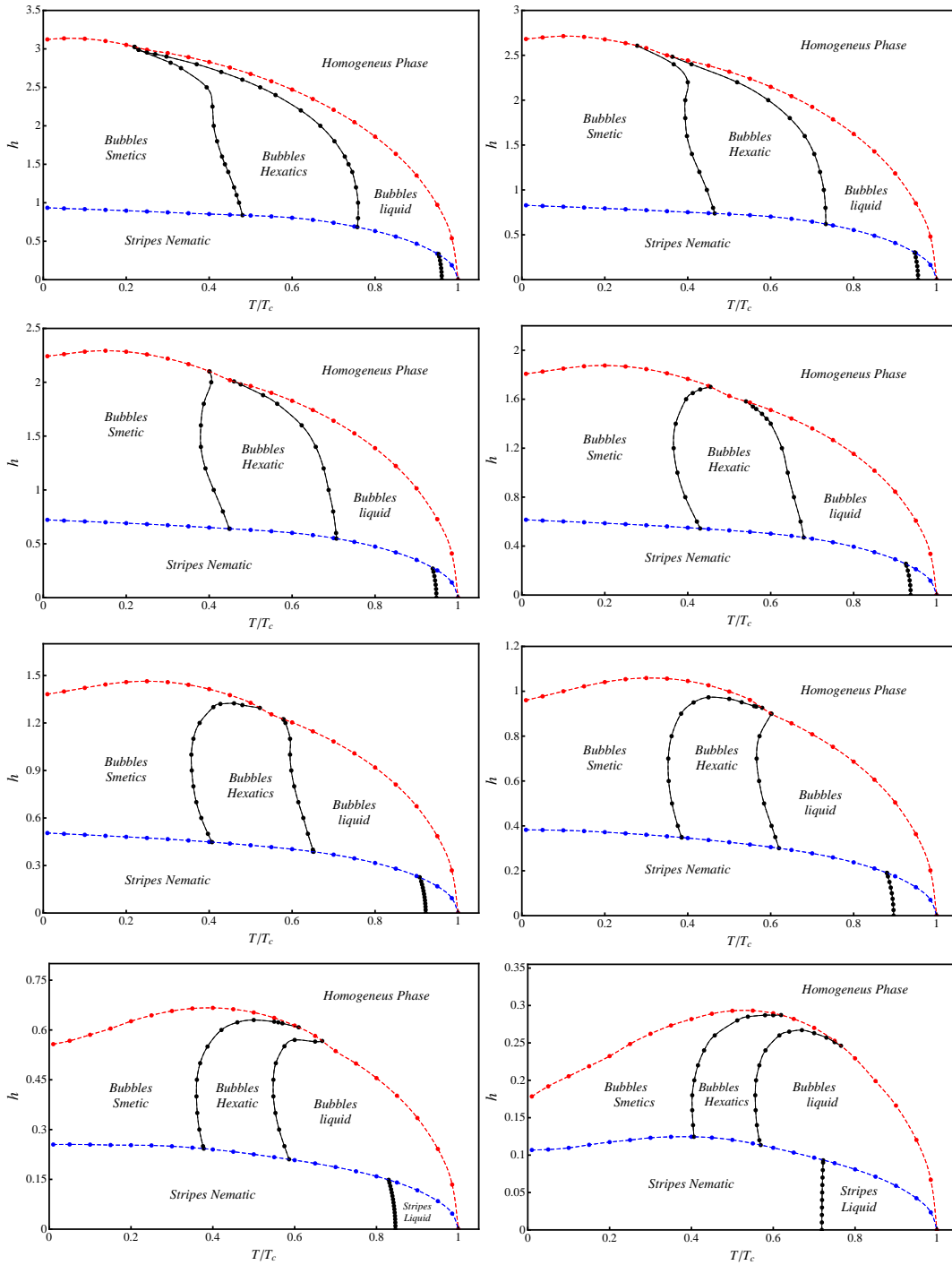


FIG. 1:  $H$ - $T$  topological phase diagrams varying the curvature of the fluctuation spectrum  $a$ . From top to bottom and left to right the values are  $a = 4.0, 3.5, 3.0, 2.5, 2.0, 1.5, 1.0, 0.5$ . In all phase diagrams three phases with broken symmetries can be identified: nematic, smectic and hexatic. All other phases are topologically equivalent since the rotational and translational symmetries are preserved.

## V. CRITICAL PROPERTIES OF THE TOPOLOGICAL TRANSITIONS

Although the critical properties are well understood in the context of KTHNY theory considering temperature as the tuning parameter, no predictions are available for the relevant quantities varying the magnetic field, mainly because there is no analog to

this parameter in the original models. Thus, a first inquire is that of the value of the critical nematic temperature at zero magnetic field  $T_N$ .

Fig. 2 shows the numerical result obtained for  $T_N$  varying the curvature of the fluctuation spectrum  $a$ . Confirming the expectations, the increase of the curvature of the fluctuation spectrum, maintaining the position of the minimum  $\hat{A}(k)$ , increases the value of  $T_N$ . In the limit of large values of  $a$  the nematic transition temperature approaches the mean field critical temperature. Considering that in our effective model it exists only one free parameter ( $a$ ) the curve presented is universal, since any microscopic Hamiltonian like that of Eq. (1) can be mapped into an effective Hamiltonian of the form of Eq. (7) and will correspond to a single value of  $a$  and  $\hat{A}(k_0)$ .

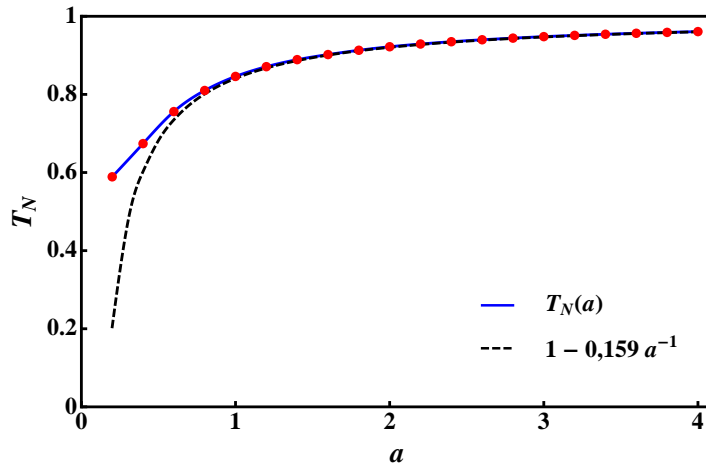


FIG. 2: Nematic critical temperature  $T_N$  at zero field varying the curvature of the fluctuation spectrum  $a$ . Dots represent the numerical results, while the dashed line corresponds to the best fit by a functionality of the form  $T_N(a) = 1 - ca^{-1}$ . For large values  $a \rightarrow \infty$  the nematic transition approaches the mean-field critical temperature.

Regarding the characterization of the form of the nematic phase boundary (nematic to stripe liquid) at low external fields, we found that the critical field  $h_c$  varies with temperature following a law of the form  $h_c \propto |T_c - T|^{1/2}$ . This kind of behavior can be understood considering that, as discussed before, the topological transitions occur at specific values of the relevant stiffness normalized by the thermal energies ( $K(0)$ ,  $K_s(0)$ ,  $K_h(0)$ ). In the case of the nematic transition, the fact that this transition occurs within the stripe region allows to conclude that  $K(0, H, T)$  have to be an even function of  $H$ , so that  $K(0, H, T) = K(0, -H, T)$ . This property can be deduced once it is recognized that the mean-field free energy is an even function of  $H$ . In the region of low fields we can expand  $K(0, H, T)$  around the point  $(T_N, 0)$  obtaining

$$K(0, H, T) = K(0, 0, T_N) + \partial_T K(0, 0, T_N)(T - T_N) + \frac{1}{2} \partial_H^2 K(0, 0, T_N) H^2 \quad (25)$$

In this way the solution of the equation  $K(0, H, T) = K(0, 0, T_N)$  will be

$$H = \left( -\frac{2\partial_T K(0, 0, T_N)(T - T_N)}{\partial_H^2 K(0, 0, T_N)} \right)^{1/2} \quad (26)$$

which explains the form of the observed curves of  $H$  versus  $T$  for the nematic boundary at low external fields.

With varying the curvature of the fluctuation spectrum  $a$  we observe a change in the shape of the nematic phase boundary (see Fig. 1). In Fig. 3 the nematic boundary is shown for two different cases: one in which the boundary behaves as expected with  $h_c(T)$  monotonically decreasing (blue curve), and one with  $h_c(T)$  monotonically increasing (red curve), in which a reentrance of the disordered phases appears with varying the external field. We realize that even in the anomalous case the field-temperature scaling does not change, as expected from Eq. (26).

An important feature of the boundary between topological phases in the phase diagrams is that they are formed by actual critical points. The external field do not break the symmetries of the modulated patterns and consequently we have the possibility of a spontaneous symmetry breaking varying both temperature and magnetic field. The critical properties varying temperature are those from KTHNY theory at any point of the boundary between the topological phases. However, the critical properties varying the magnetic field are not obvious.

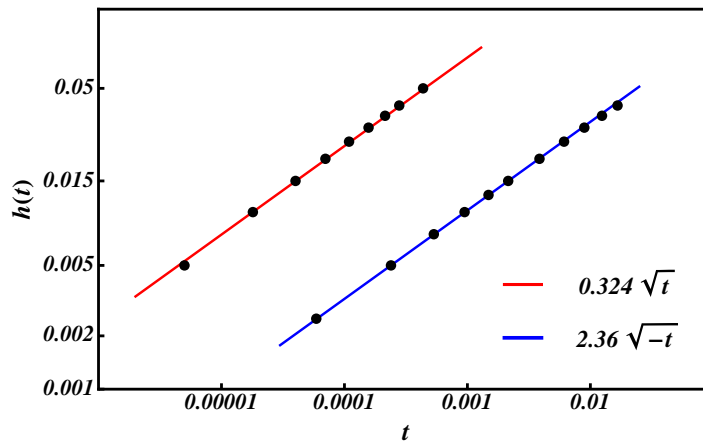


FIG. 3: Critical nematic field  $h_c(t)$  varying the reduced temperature ( $t = T - T_N(a)$ ) for fluctuation spectrum curvatures  $a = 2.5$  (blue)  $a = 0.2$  (red). For  $a = 2.5$  there is a normal  $h_c(t)$  behavior while for  $a = 0.2$ , reentrance exists varying the external field.

Following previous arguments on the local behavior of  $K(0, H, T)$  it can be shown that the critical properties varying the external field depend on the local form of the topological phase boundary. Without loss of generality, let's consider an arbitrary point of the nematic phase boundary  $(H_0, T_0)$ . Since  $K(0, H, T)$  is an analytic function in the  $H$ - $T$  plane, the series expansion in powers of  $(T - T_0)$  and  $(H - H_0)$  have the form

$$K(0, H, T) = K(0, 0, T_N) + \partial_T K(0, H_0, T_0)(T - T_0) + \frac{1}{n!} \partial_H^n K(0, H_0, T_0)(H - H_0)^n, \quad (27)$$

where only the leading order terms in  $(T - T_0)$  and  $(H - H_0)$  are kept,  $n$  represents the order of the lowest external field contribution and the relation  $K(0, H_0, T_0) = K(0, 0, T_N)$  have been used. Around the point  $(H_0, T_0)$  the solution of the equation  $K(0, H, T) = K(0, H_0, T_0)$  have the form

$$H - H_0 = \left( -\frac{n! \partial_T K(0, H_0, T_0)(T - T_0)}{\partial_H^n K(0, H_0, T_0)} \right)^{1/n}. \quad (28)$$

At the same time, studying the variations of  $K(0, H, T)$  around  $(H_0, T_0)$  by fixing  $T$  or  $H$  it can be seen that the critical exponents varying the external field  $\nu_h$  are related to those varying temperature  $\nu_T$  in the form  $\nu_h = n\nu_T$ . This means that the critical properties varying temperature and varying the external field can be related by just looking at the form of the topological phase boundary. The arguments raised here for the nematic phase are valid for the smectic and the hexatic phases as well.

To further illustrate this argument it is presented in Fig. 4 the numerical calculation of the behavior of the nematic and the smectic correlation lengths as function of the external field for two points of the respective phase boundaries. Since at the selected critical points the phase boundary is not vertical it is natural to expect that the critical behavior varying the external field coincides with that varying temperature.

## VI. CONCLUSIONS

We have studied the full topological phase diagram of a model of ultrathin dipolar ferromagnetic layer in the limit of strong perpendicular anisotropy. These type of systems have been already experimentally synthesized and the relevance of the present work leans partially on this fact<sup>21,22</sup>. Our theoretical analysis suggest the existence of several topological phases within the stripe and the bubble regions of the  $H$ - $T$  diagrams. Although experimental observation and characterization of such intermediate phases is a challenge by itself, the state of the art in magnetic measurement techniques<sup>32</sup> allows in principle a topological characterization of the phases of the magnetic textures considered here.

The existence of such exotic phases in magnetic systems is quite interesting because what intuition may suggest is that the temperature would only produce local fluctuations in a way that, either the thermal fluctuations are weak enough to be unable to destroy the magnetic texture or they are just strong enough to destroy the magnetic pattern at once. This scenario would be only consistent with the occurrence of a single transition from the low temperature ordered phase to the paramagnetic phase, as is

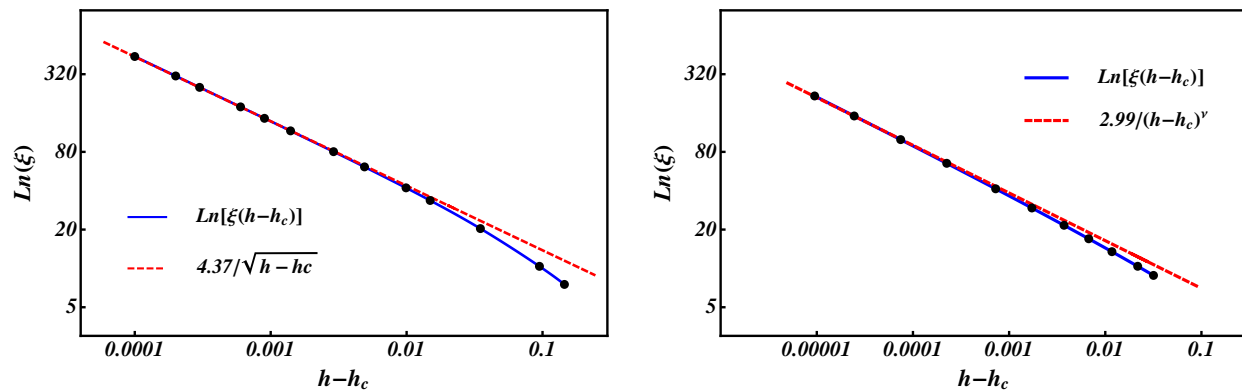


FIG. 4: Nematic (Left) and smectic (Right) correlation lengths varying the external field for  $a = 2.5$  at  $T = 0.937$  and  $T = 0.4$  respectively. The estimated critical fields at those temperatures are  $h_c = 0.0551001$  and  $h_c = 0.7582755$  respectively. The critical exponent of the smectic transition at the temperature considered is  $\nu = 0.36963477$  in agreement with the classical theory of melting.

normally predicted by mean-field theories. Instead, what we find is the occurrence of intermediate topological phases including “liquid” states, in which the magnetic textures fluctuate and move as robust structures. These states are particularly interesting since the motion of these structures occurs without any mass transportation.

We additionally establish the relation between the strong reentrance of the homogeneous phase and the existence of anomalous or reentrant topological transitions. The relation between these two features can be understood in terms of a considerable growth of the modulation length as the external field is increased, producing an anomalous behavior of the elastic constant of the magnetic patterns<sup>33,34</sup>.

#### Acknowledgments

We gratefully acknowledge useful discussions with Mats Wallin and Jack Lidmar, partial financial support from CNPq (Brazil) and the Laboratório de Física Computacional from IF-UFRGS for the use of the cluster Ada. R.D.M. acknowledges the Swedish Research Council Grants No. 642-2013-7837, 2016-06122, 2018-03659 and Göran Gustafsson Foundation for Research in Natural Sciences and Medicine and Olle Engkvists Stiftelse.

- 
- \* Electronic address: alejandro.mendoza@ufsc.br
- <sup>1</sup> I. Booth, A. B. MacIsaac, J. P. Whitehead, and K. De’Bell, Phys. Rev. Lett. **75**, 950 (1995).
  - <sup>2</sup> D. Sornette, J. Physique **48**, 151 (1987).
  - <sup>3</sup> D. Andelman, F. Brochard, and J. F. Joanny, J. Chem. Phys. **86**, 3673 (1987).
  - <sup>4</sup> R. Allenspach, M. Stampanoni, and A. Bischof, Phys. Rev. Lett. **65**, 3344 (1990).
  - <sup>5</sup> S. A. Cannas, M. Carubelli, O. V. Billoni, and D. A. Stariolo, Phys. Rev. B **84**, 014404 (2011).
  - <sup>6</sup> S. Pighín, O. V. Billoni, D. A. Stariolo, and S. A. Cannas, J. Mag. Mag. Mat. **322**, 3889 (2010).
  - <sup>7</sup> A. Deutsch and S. A. Safran, Phys. Rev. E **54**, 3906 (1996), URL <http://link.aps.org/doi/10.1103/PhysRevE.54.3906>.
  - <sup>8</sup> N. D. Mermin and H. Wagner, Phys. Rev. Lett. **17**, 1133 (1966).
  - <sup>9</sup> D. R. Nelson, Phys. Rev. B **18**, 2318 (1978), URL <https://link.aps.org/doi/10.1103/PhysRevB.18.2318>.
  - <sup>10</sup> J. M. Kosterlitz and D. J. Thouless, Journal of Physics C: Solid State Physics **6**, 1181 (1973).
  - <sup>11</sup> J. Toner and D. R. Nelson, Phys. Rev. B **23**, 316 (1981).
  - <sup>12</sup> A. Abanov, V. Kalatsky, V. L. Pokrovsky, and W. M. Saslow, Phys. Rev. B **51**, 1023 (1995).
  - <sup>13</sup> D. G. Barci and D. A. Stariolo, Phys. Rev. Lett. **98**, 200604 (2007).
  - <sup>14</sup> R. Díaz-Méndez, A. Mendoza-Coto, R. Mulet, L. Nicolao, and D. Stariolo, Eur. Phys. J. B **81**, 309 (2011), ISSN 1434-6028, URL <http://dx.doi.org/10.1140/epjb/e2011-20185-y>.
  - <sup>15</sup> A. Mendoza-Coto, D. A. Stariolo, and L. Nicolao, Phys. Rev. Lett. **114**, 116101 (2015), URL <http://link.aps.org/doi/10.1103/PhysRevLett.114.116101>.
  - <sup>16</sup> L. Nicolao, A. Mendoza-Coto, and D. A. Stariolo, Journal of Physics: Conference Series **686**, 012005 (2016), URL <http://stacks.iop.org/1742-6596/686/i=1/a=012005>.
  - <sup>17</sup> J. M. Kosterlitz, Rep. Prog. Phys. p. 026001 (2016).

- <sup>18</sup> T. Garel and S. Doniach, *Phys. Rev. B* **26**, 325 (1982).
- <sup>19</sup> K. De’Bell, A. B. MacIsaac, and J. P. Whitehead, *Rev. Mod. Phys.* **72**, 225 (2000).
- <sup>20</sup> K. De’Bell, A. B. MacIsaac, I. N. Booth, and J. P. Whitehead, *Phys. Rev. B* **55**, 15108 (1997).
- <sup>21</sup> O. Portmann, A. Vaterlaus, and D. Pescia, *Nature* **422**, 701 (2003).
- <sup>22</sup> N. Saratz, A. Lichtenberger, O. Portmann, U. Ramsperger, A. Vindigni, and D. Pescia, *Phys. Rev. Lett.* **104**, 077203 (2010).
- <sup>23</sup> B. I. Halperin and D. R. Nelson, *Physical Review Letters* p. 121 (1978).
- <sup>24</sup> D. R. Nelson and B. I. Halperin, *Phys. Rev. B* **19**, 2457 (1979), URL <https://link.aps.org/doi/10.1103/PhysRevB.19.2457>.
- <sup>25</sup> A. P. Young, *Phys. Rev. B* p. 191855 (1979).
- <sup>26</sup> A. Mendoza-Coto, L. Nicolao, and R. Díaz-Méndez, *Scientific Reports* **9** (2019), URL <https://doi.org/10.1038/s41598-018-38465-8>.
- <sup>27</sup> S. A. Pighín and S. A. Cannas, *Phys. Rev. B* **75**, 224433 (2007).
- <sup>28</sup> R. Díaz-Méndez and R. Mulet, *Phys. Rev. B* **81**, 184420 (2010).
- <sup>29</sup> A. Mendoza-Coto, O. V. Billoni, S. A. Cannas, and D. A. Stariolo, *Phys. Rev. B* **94**, 054404 (2016), URL <https://link.aps.org/doi/10.1103/PhysRevB.94.054404>.
- <sup>30</sup> A. Mendoza-Coto, D. A. Stariolo, and L. Nicolao, *Phys. Rev. Lett.* **117**, 239602 (2016), URL <https://link.aps.org/doi/10.1103/PhysRevLett.117.239602>.
- <sup>31</sup> A. Kashuba and V. L. Pokrovsky, *Phys. Rev. Lett.* **70**, 3155 (1993), URL <https://link.aps.org/doi/10.1103/PhysRevLett.70.3155>.
- <sup>32</sup> M. Kronseider, T. N. G. Meier, M. Zimmermann, M. Buchner, M. Vogel, and C. H. Back, *Nature Communications* **6** (2015).
- <sup>33</sup> O. Portmann, A. Gölzer, N. Saratz, O. V. Billoni, D. Pescia, and A. Vindigni, *Phys. Rev. B* **82**, 184409 (2010).
- <sup>34</sup> A. Mendoza-Coto and D. A. Stariolo, *Phys. Rev. E* **86**, 051130 (2012), URL <https://link.aps.org/doi/10.1103/PhysRevE.86.051130>.